Desalination and Water Treatment
www.deswater.com
doi: 10.5004/dwt.2023.29283

285 (2023) 113–120
February

Removal of natural organic matter on the oxidation and coagulation of ferrate: role of Ca

Wentao Li[a], Xuemi Huang[a], Guangyu An[b], Jianning Guo[a], Runsheng Zhong[a,*], Feng Xiao[a,c], Dongsheng Wang[b]

[a]*Shenzhen Institute of Information Technology, Shenzhen 518172, China, emails: zhongrs@sziit.edu.cn (R.S. Zhong), liwentao318@126.com (W.T. Li), 2947883922@qq.com (X.M. Huang), 154136751@qq.com (J.N. Guo)*
[b]*Research Center for Eco-Environmental Sciences, Chinese Academy of Sciences, Beijing 100085, China, email: 499733235@qq.com (G.Y. An), wgds@rcees.ac.cn (D.S. Wang)*
[c]*School of Renewable Energy, North China Electric Power University, Beijing 102206, China, email: fengxiao@reecs.ac.cn (F. Xiao)*

Received 14 September 2022; Accepted 25 December 2022

ABSTRACT

The natural organic matter (NOM) contaminated water treated by ferrate without or with Ca ions was comparatively studied. The NOM removal process by ferrate assisted with kaolin clay were investigated under different NOM concentration. At pH 9.0, the NOM removal by ferrate with Ca could significantly improve 55% than without Ca, and Ca could promote the transformation of ferrate to iron oxides instead of soluble Fe. The flocs produced from NOM removal by ferrate without or with Ca was analysed by fractal dimension and Fourier-transform infrared spectroscopy. We found that Ca could increase the strength and recovery of flocs structure in the NOM removal process by ferrate. Therefore, Ca addition can enhance the oxidation and coagulation of ferrate in the water treatment.

Keywords: Ferrate; Coagulation; Oxidation; Ca; Natural organic matter

1. Introduction

The natural organic matter (NOM), ubiquitously existing in natural waters, is a very diverse collection of organic molecules derived from natural sources [1–2]. The presence of NOM in surface water are highly concerned. Because NOM can bring a few problems for drinking water: (1) poor aesthetic quality of the water such as colour, taste, odour [1,3–4]; (2) potential health risk due to the formation of disinfection by-products (DBPs) during water treatment by reacting with other chemicals [5–7]; (3) bacterial regrowth and biofilm formation in distribution systems [1,3]. Therefore, it's quite important to the elimination and control of NOM levels.

The most applied methods for removal of NOM from water are coagulation [8–10], adsorption [10,11], membrane filtration [12,13], advanced oxidation processes (AOPs) [7,14,15], biological and ion exchange (IE) processes [1,16,17]. Coagulation and flocculation for NOM removal from drinking water has recently attracted significant attention from scientists and industry, because of low cost and short time [9,18]. In the coagulation process, coagulants are critical to improve the NOM removal efficiency, including ferric salts and aluminium salts. Köhler et al. [19] reported that 50%–52% of NOM was removed by coagulation/sedimentation and filtration at the Gorvaln WTP in Sweden. To improve the NOM removal efficiency, oxidants (e.g., liquid chlorine, pypocholoride, ozone) are used as pretreatment and

* Corresponding author.

followed by coagulation. These oxidants can often react with NOM, producing new aromatic halogenated DBPs [20,21].

Ferrate often has been used as a high-effective and green chemical agent for removing various organic contaminants [22,23]. The advantage of the application of ferrate arises from oxidation and subsequent coagulation by γ-Fe_2O_3 serving as an in situ coagulant and adsorbent [24]. There is a handful studies reported in the literatures on the effective oxidation and coagulation of pharmaceuticals and other contaminants such as different disinfection by-product precursors [25,26]. Several researchers have investigated that heavy metals (e.g., Fe(II), Fe(III), Mn(II)) and silica gel could enhance the degradation of pharmaceuticals in the wastewater by ferrate [27,28]; however, the effect of surface water quality (e.g., Ca ion and clay particles) on the oxidation and coagulation of ferrate to remove NOM is largely unknown. Therefore, there is an urgent need to investigate the efficient and environmentally friendly technologies for the removal of NOM in aquatic environment.

The objectives of this work were (1) to compare the NOM removal efficiency and molecular weight by ferrate with or without Ca; (2) to investigate the effect of Ca on the fractal structure and particle size of flocs; (3) to analyze the floc structure by Fourier-transform infrared spectroscopy (FTIR).

2. Materials and methods

2.1. Materials and reagents

Potassium ferrate (K_2FeO_4, >99%), humic acid (HA, >90%), calcium chloride ($CaCl_2$, >99%), sodium bicarbonate ($NaHCO_3$, >99%) and kaolin (1–5 um, negative charge) were purchased from Sigma-Aldrich or Sinopharm Chemical Reagent Co., Ltd. All the solutions were prepared by using ultrapure water (Mill-Q Biocel, 18 MΩ).

Stock solution was prepared as follows: 1.00 g humic acid was dissolved in 1 L of 1×10^{-3} mol/L NaOH solution with 24 h of continuous stirring, and then filtered through 0.45 um glass fiber membrane filter. 1.00 g kaolin was dissolved in 1 L ultrapure water and stirred for 24 h. 0.2 mol/L $NaHCO_3$ was also prepared. These solutions were stored in refrigerator for later use.

Synthetic test NOM water was prepared by adding a measured amount of humic acid stocking solution into deionized water (0–40 mg/L TOC), meanwhile, 1.0 mmol/L $NaHCO_3$ was added to provide a certain buffer capacity and ionic strength as well as 50 mg/L kaolin. The pH of test water was adjusted by 0.1 mol/L NaOH or 0.1 mol/L HNO_3 solutions.

2.2. Jar tests

Flocs were formed by performing a series of jar tests. After 10 min of slow growth phase, the mixing speed was increased to 200 rpm for 1 min to break the flocs, followed by another slow mixing at 40 rpm for 10 min to regrow the flocs. A laser diffraction instrument (Malvern Mastersizer 2,000, Malvern, U.K.) was used to measure the median d_{50} floc size during the whole experiment. The suspension was monitored by drawing water through the optical unit of the Mastersizer and back into the jar by a peristaltic pump on the return tube with 6 mm internal diameter peristaltic pump tubing. The inflow and outflow tubes were positioned opposite one another at a depth just above the paddle in the holding ports. Ferrate and pH adjustment chemicals were added at the start of the rapid mix. Size measurements were taken every 30 s for the duration of the jar test and logged onto a computer. Flocs were pumped through the system at a flow rate of 10 rpm.

Standard jar tests were conducted on a program-controlled jar test apparatus (TA-6, Wuhan Hengling Technology Co., Ltd., China) at room temperature. Test water of 300 mL was transferred into a 500 mL beaker; under rapid stirring of 250 rpm for 0.5 min, 0.2 mmol/L ferrate was dosed to pre-oxidation, followed by a rapid mix at 200 rpm for 1 min; after 1.5 min, the stirring speed was changed to 40 rpm with a duration of 10 min; then after 30 min of quiescent string, sample was collected from 2 cm below the surface for measurements. Collected sample was filtered through 0.45 um membrane to measure total organic carbon (TOC), final pH, and turbidity.

2.3. Analysis

Infrared spectrums were recorded on a Thermo Fisher Nicolet 8700 ATR-FTIR spectrometer. The pH of all solutions was read by a Mettler Toledo pH meter (FE20) with a combined glass electrode (LE438). The turbidity was measured using a 2100 N turbidimeter (Hach, USA). The TOC of the solution was analyzed using a TOC-VCPH analyzer (Shimadzu, Japan). The molecular weight of NOM was determined using high performance liquid chromatography (1200 series; Agilent) with a C18 column (5 μm, 4.6 × 250 mm; Agilent). The analysis was carried out at 254 nm using a H_3PO_4 solution (pH = 3) as the mobile phase.

3. Results

3.1. Removal of NOM with ferrate

The TOC removal efficiency, turbidity and Fe residual amount on the NOM removal by ferrate were investigated at pH 7.0. Fig. 1 shows the variation of NOM removal efficiency, turbidity and Fe residual amount as a function of the increase of NOM concentration. In the process of NOM removal by ferrate, when NOM content was increased from 0 to 18.8 mg·C/L, the NOM removal efficiency and turbidity in solution was 80%–100% and 2–30 NTU, respectively, with the increase from 0 to 4 mg/L of Fe residual amount. When NOM was increased from 18.79 to 37.58 mg·C/L, TOC removal efficiency was decreased from 80% to about 0%, and turbidity and Fe residual amount were increased from 30 to 80 NTU and from 4 to 12 mg/L, respectively. This indicates ferrate can completely remove NOM with less than 18.79 mg/L at pH 7.0. Compared with NOM removal by Fe salt (Fig. S1), for moderate HA concentration (10–20 mg/L), the NOM removal efficiency from ferrate was high 4–5 times than that from Fe salt coagulation. This may be related with the oxidation of ferrate.

The change of 0–40 mg·C/L NOM molecular weight before and after ferrate treatment is shown in Fig. 2. The results display that most NOM molecular weights were

1–10 K. At less than 10 mg·C/L NOM, few molecules using ferrate treatment were left compared with Fe salt treatment (Fig. S2). At moderate concentration (18.79 mg·C/L), most of molecules were removed by ferrate while some molecules (2 K–8 kDa) were left by Fe salt treatment. At high concentration (37.58 mg·C/L), large amounts of molecules were left after ferrate treatment, even producing more large molecular weights (40 kDa). This mainly resulted from colloid particles [29,30], indicating that iron oxides were coated by parts of organic molecules.

3.2. Impact of Ca on the NOM removal by ferrate

The variations of TOC removal efficiency, Ca concentration and Fe residual on the NOM removal by ferrate with Ca at pH 9.0 are shown in Figs. 3 and S3. In the removal process of 10.3 mg·C/L NOM, with the increase of Ca from 0 to 0.75 mmol/L, TOC removal efficiency was up from 0% to about 55%, and Ca was almost no adsorbed. Interestingly, Fe residual concentration was decreased from about 9 mg/L to 0. For high NOM concentration (around 21 mg·C/L), the removal behaviors in Fig. S3 were similar with those in low NOM. For example, increasing the Ca concentration from 0 to 0.75 mmol/L, TOC was decreased from 21 to 17 mg·C/L, the Fe residual amount decreased from around 10 to 8.5 mg/L, and Ca concentration was no changed. This indicates that Ca may remarkably affect the oxidation and coagulation of ferrate.

The NOM molecular weight distribution after treatment by ferrate with or without Ca at pH 9.0 is shown in Fig. 4. At low Ca concentration (0–0.30 mmol/L Ca), all the molecules were almost no removed, producing more large molecular weights (40 kDa).In contrast, high Ca concentration (0.75 mmol/L Ca) can promote the NOM molecular removal and avoid the formation of large molecular weights (40 kDa).

3.3. Flocs analysis of NOM and Ca with ferrate

3.3.1. Fractal dimension analysis

The influence of Ca^{2+} and NOM on floc growth at ferrate dosage 0.2 mmol/L and pH 7.0 is shown in Fig. 5. The

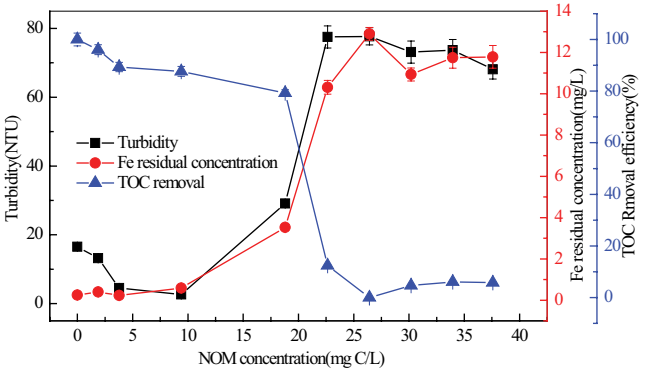

Fig. 1. Fe concentration and remaining turbidity, TOC removal efficiency in the solution during the NOM removal by ferrate (ferrate dosage: 0.2 mmol/L; NOM concentration: 0–40 C·mg/L; kaolin dosage: 50 mg/L; pH: 7.0).

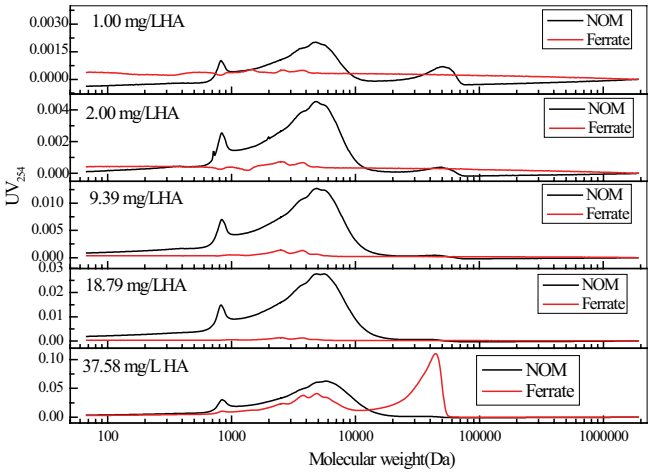

Fig. 2. NOM molecular weight distribution after ferrate treatment.

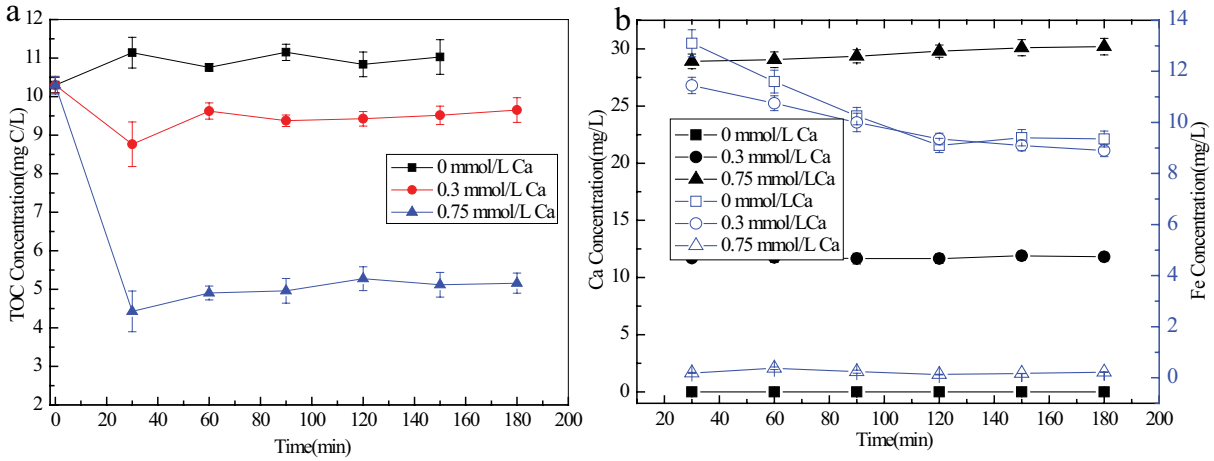

Fig. 3. TOC removal efficiency, Fe concentration and Ca concentration in the solution during the NOM removal by ferrate (ferrate dosage: 0.2 mmol/L; NOM concentration: 10.3 mg/L; Ca dosage: 0–0.75 mmol/L; pH: 9.0).

results show that NOM was better able to accelerate the ferrate coagulation than Ca^{2+}. In Fig. 6A, by increasing NOM concentration, flocs size and growth rate rose and then fell. For instance, flocs size kept growing to achieve the largest medium diameter (around 650 um) at 16 mg·C/L of NOM concentration; flocs growth rate reached the highest value (650 um/min) at 8 mg·C/L of NOM concentration. In Fig. 6B, flocs size (250–300 um) and growth rate (80–100 um/min) were less changed after the addition of Ca^{2+} compared with the addition of NOM.

The aggregates' structure can be simply described by a parameter D_f, fractal dimension, which was defined as the exponent of relationship of mass (M) and size (L) [13]:

$$M_f \propto L^{D_f} \tag{1}$$

Similar relationships can be obtained regarding the volume and sedimentation velocity to particle size. In Fig. 6C and D, there was almost no difference in Fe flocs fractal dimension (D_f) when breakage or regrowth, but NOM or Ca had large influence on the Fe flocs fractal dimension. For example, the D_f of Fe flocs increased to around 2.50 at 20 mg/L of NOM and then reduced with increasing their concentrations. With the increase of Ca concentration, Fe floc fractal dimension was increased from 2.25 to 2.35. In 0.2 mmol/L ferrate dosage, Fe flocs size, growth rate and fractal dimension were increased when NOM reaching 8–16 mg·C/L, and then decreased; they were no significantly changed with the increase of Ca concentration. As having been reported in the previous studies [31,32], flocs with open structure have low D_f values, whereas, high D_f values generally indicate more compact structures.

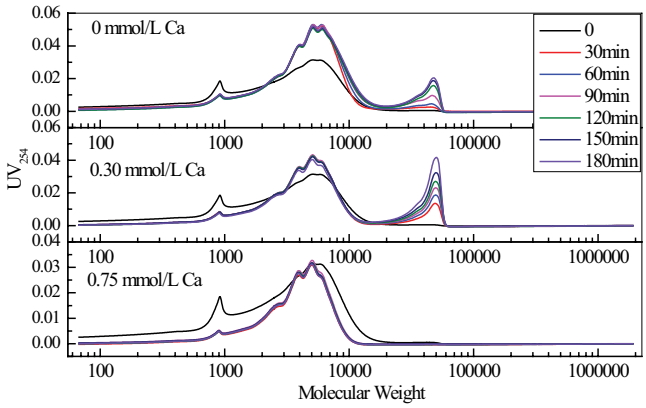

Fig. 4. NOM molecular weight distribution after treatment by ferrate with Ca.

The strength factor and recovery factor calculated using Eqs. (2) and (3) in Table 1 were used to interpret the floc breakage and recoverability. The addition of NOM decreased the strength factor value (58) and recovery factor value (23) at 4 mg·C/L. By increasing NOM concentration, the recovery factor value of flocs was decreased from 50 to 12 while strength factor value was increased slightly. In contrast, Ca could improve the recovery factor and strength factor that were 73 and 60 at 1.0 mmol/L of Ca. This suggested that flocs with Ca were similar to resist shear with NOM, and the regrowth of flocs with NOM was poorer than that with Ca.

$$\text{Strength factor} = \frac{d_2}{d_1} \times 100 \tag{2}$$

$$\text{Recovery factor} = \frac{d_3 - d_2}{d_1 - d_2} \times 100 \tag{3}$$

3.3.2. Flocs structure analysis

FTIR spectra of Fe flocs obtained by ferrate were measured. FTIR of kaolin (Fig. S4) showed usual peaks at 1,114; 1,025 and 996 cm^{-1} for Si–O bending [33,34], 934 and 909 cm^{-1} for Al–OH bending [33], 789 and 749 cm^{-1} for Si–O–Al compounded vibrations [34]. Fig. 7 exhibits the FTIR spectra of

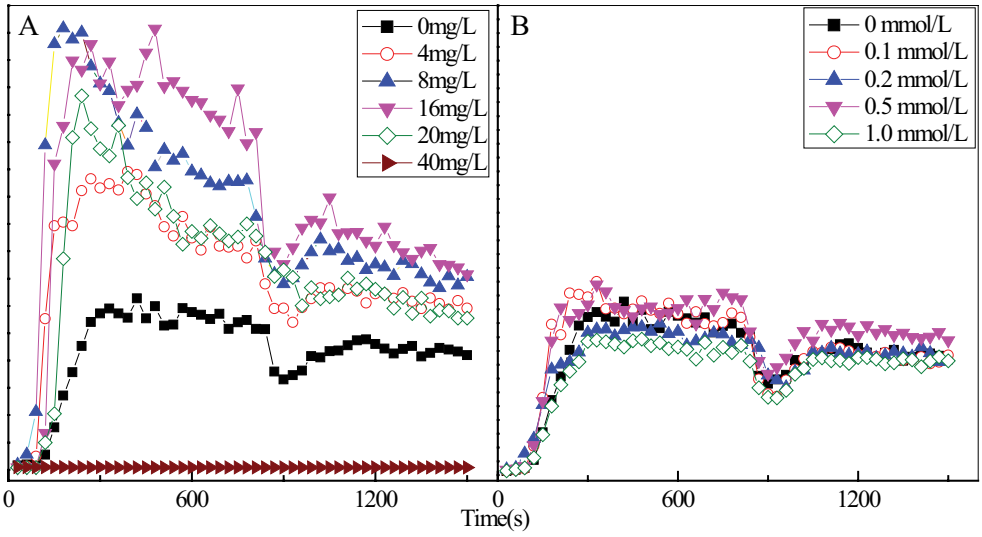

Fig. 5. The growth, breakage and regrowth profiles of ferrate flocs with NOM or Ca at pH 7.0 (A) [NOM] = 0–40 mg·C/L and (B) [Ca^{2+}] = 0–1.0 mmol/L).

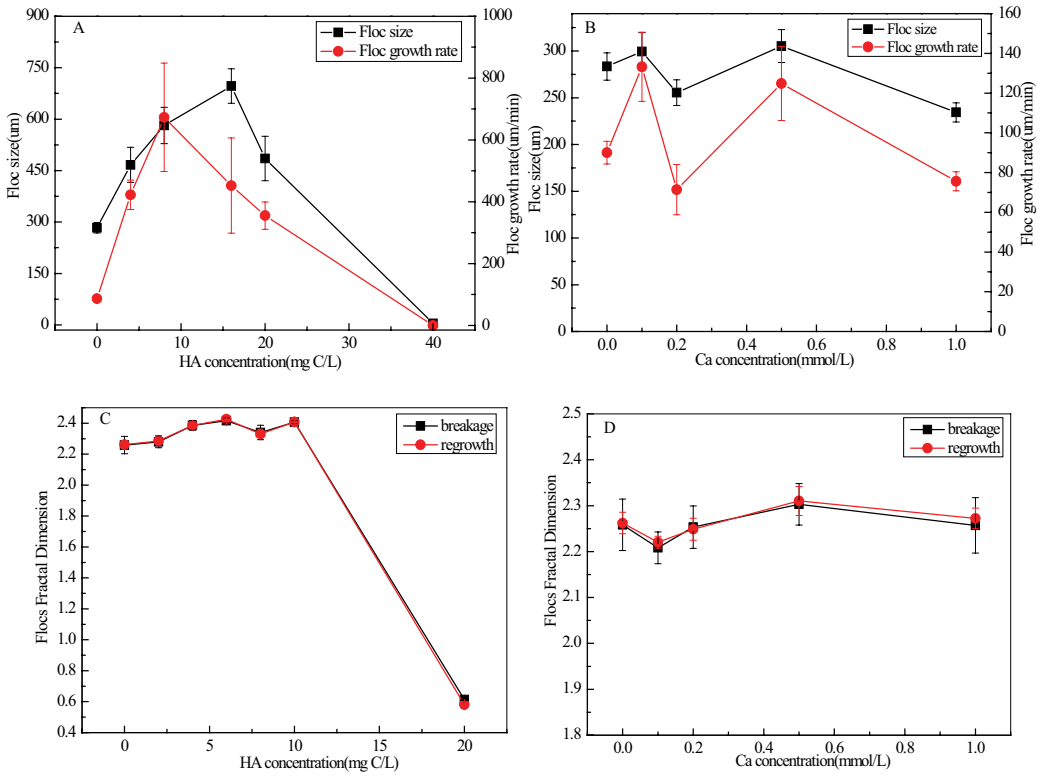

Fig. 6. Change in flocs growth rate (0–5 min), flocs size (5–12 min) and flocs fractal dimension (breakage and regrowth) of flocs with different Ca concentration or NOM concentration (A,C) NOM and (B,D) Ca^{2+}.

Table 1
Strength and recovery factors of flocs formed with different solvents after breakage

Solvent	Concentration	Strength factor	Recovery factor
	0	58	50
NOM	4 mg·C/L	58	23
	8 mg·C/L	58	12
	16 mg·C/L	54	12
	20 mg·C/L	62	12
Ca	0.1 mmol/L	48	51
	0.2 mmol/L	62	65
	0.5 mmol/L	60	66
	1.0 mmol/L	60	73

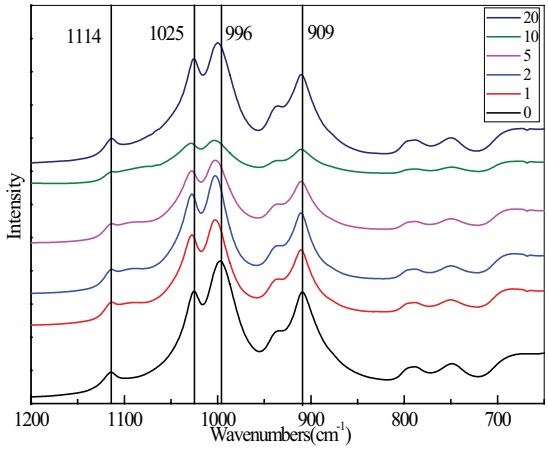

Fig. 7. FTIR spectra of flocs produced from 0.2 mmol/L ferrate with 50 mg/L kaolin under different NOM concentration.

Fe flocs produced from ferrate under different NOM concentrations. In the absence of NOM, the IR spectra of flocs obtained from ferrate was almost the same with that of kaolin. As seen from Fig. 7, by the increase of NOM concentration from 0 to 10 mg/L, the peaks of 996 and 1,025 cm^{-1} at the IR of Fe-NOM flocs from ferrate also shifted to high wavenumbers and their intensities were decreased, suggesting that the Si–O–Fe binding was formed. When the NOM concentration reached 20 mg/L, the peak of 1,025 cm^{-1} returned the initial position. This attributes that more NOM inhibits the interaction between kaolin particles and iron oxides producing by decomposition of ferrate.

4. Conclusion

In summary, this study mainly includes as follows: The comparison of NOM removal by ferrate in the presence of Ca or not was studied. The removal efficiency of NOM (around 20 mg·C/L) by ferrate at pH 7.0 was 4–5 times than that by Fe salts; Ca addition can significantly improve 55%

for NOM removal by ferrate at pH 9.0 and inhibit the transformation of iron oxides to soluble Fe. The flocs produced from NOM removal by ferrate without or with Ca was analyzed by fractal dimension and FTIR. We found that Ca could increase the strength and recovery of flocs structure in the NOM removal process by ferrate.

Acknowledgement

The authors acknowledge the supports by the Youth Innovative Talent Project from College and University in Guangdong Province (no.2018GkQNCX081), and Shenzhen Institute of Information Technology Project (SZIIT2021KJ026).

References

[1] J. Winter, H.E. Wray, M. Schulz, R. Vortisch, B. Barbeau, P.R. Bérubé, The impact of loading approach and biological activity on NOM removal by ion exchange resins, Water Res., 134 (2018) 301–310.
[2] M. Amano, J. Lohwacharin, A. Dubechot, S. Takizawa, Performance of integrated ferrate–polyaluminum chloride coagulation as a treatment technology for removing freshwater humic substances, J. Environ. Manage., 212 (2018) 323–331.
[3] A. Keucken, X.F. Liu, B.Y. Lian, Y. Wang, K.M. Persson, G. Leslie, Simulation of NOM removal by capillary NF: a numerical method for full-scale plant design, J. Membr. Sci., 555 (2018) 229–236.
[4] M. Kumar, H.M. Baniowda, N. Sreedhar, E. Curcio, H.A. Arafat, Fouling resistant, high flux, charge tunable hybrid ultrafiltration membranes using polymer chains grafted graphene oxide for NOM removal, Chem. Eng. J., 408 (2021) 127300, doi: 10.1016/j.cej.2020.127300.
[5] I. Levchuk, J.J.R. Márquez, M. Sillanpää, Removal of natural organic matter (NOM) from water by ion exchange – a review, Chemosphere, 192 (2018) 90–104.
[6] R. Sudoh, M.S. Islam, K. Sazawa, T. Okazaki, N. Hata, S. Taguchi, H. Kuramitz, Removal of dissolved humic acid from water by coagulation method using polyaluminum chloride (PAC) with calcium carbonate as neutralizer and coagulant aid, J. Environ. Chem. Eng., 3 (2015) 770–774.
[7] Z.C. Hua, X.J. Kong, S.D. Hou, S.Q. Zou, X.B. Xu, H. Huang, J.Y. Fang, DBP alteration from NOM and model compounds after UV/persulfate treatment with post chlorination, Water Res., 158 (2019) 237–245.
[8] H.N.P. Dayarathne, M.J. Angove, R. Aryal, H.A. Naga, B. Mainali, Removal of natural organic matter from source water: review on coagulants, dual coagulation, alternative coagulants, and mechanisms, J. Water Process Eng., 40 (2021) 101820, doi: 10.1016/j.jece.2015.04.007.
[9] C.C. Davis, M. Edwards, Role of calcium in the coagulation of NOM with ferric chloride, Environ. Sci. Technol., 51 (2017) 11652–11659.
[10] Y.P. Xu, T. Chen, Z.Q. Liu, S.J. Zhu, F.Y. Cui, W.X. Shi, The impact of recycling alum-humic-floc (AHF) on the removal of natural organic materials (NOM): behavior of coagulation and adsorption, Chem. Eng. J., 284 (2016) 1049–1057.
[11] B. Zhang, S.Y. Avsar, M.K. Corliss, M. Chung, N.J. Cho, Influence of natural organic matter (NOM) coatings on nanoparticle adsorption onto supported lipid bilayers, J. Hazard. Mater., 339 (2017) 264–273.
[12] Y.Q. Guo, H. Liang, G.B. Li, D.L. Xu, Z.S. Yan, R. Chen, J. Zhao, X.B. Tang, A solar photo-thermochemical hybrid system using peroxydisulfate for organic matters removal and improving ultrafiltration membrane performance in surface water treatment, Water Res., 188 (2021) 116482, doi: 10.1016/j.watres.2020.116482.
[13] T. Mantel, P. Benne, M. Ernst, Electrically conducting duplex-coated gold-PES-UF membrane for capacitive organic fouling mitigation and rejection enhancement, J. Membr. Sci., 620 (2021) 118831, doi: 10.1016/j.memsci.2020.118831.
[14] M. Kohantorabi, S. Giannakis, M.R. Gholami, L. Feng, C. Pulgarin, A systematic investigation on the bactericidal transient species generated by photo-sensitization of natural organic matter (NOM) during solar and photo Fenton disinfection of surface waters, Appl. Catal., B, 244 (2019) 983–995.
[15] Y. Zhang, Z.L. Lu, Z.Y. Zhang, B.Y. Shi, C. Hu, L. Lyu, P.X. Zuo, J. Metz, H.B. Wang, Heterogeneous Fenton-like reaction followed by GAC filtration improved removal efficiency of NOM and DBPs without adjusting pH, Sep. Purif. Technol., 260 (2021) 118234, doi: 10.1016/j.seppur.2020.118234.
[16] M. Schulz, J. Winter, H. Wray, B. Barbeau, P. Bérubé, Biologically active ion exchange (BIEX) for NOM removal and membrane fouling prevention, Water Sci. Technol. Water Supply, 17 (2017) 1178–1184.
[17] I. Caltran, L.C. Rietveld, H.L. Shorney-Darby, S.G.J. Heijman, Separating NOM from salts in ion exchange brine with ceramic nanofiltration, Water Res., 179 (2020) 115894, doi: 10.1016/j.watres.2020.115894.
[18] N. Xue, X. Wang, F.R. Zhang, Y. Wang, Y.B. Chu, Y. Zheng, Effect of SiO_2 nanoparticles on the removal of natural organic matter (NOM) by coagulation, Environ. Sci. Pollut. Res., 23 (2016) 11835–11844.
[19] S.J. Köhler, E. Lavonen, A. Keucken, P. Schmitt-Kopplin, T. Spanjer, K. Persson, Upgrading coagulation with hollow-fibre nanofiltration for improved organic matter removal during surface water treatment, Water Res., 89 (2016) 232–240.
[20] X. Wang, J. Wang, Y. Zhang, Q. Shi, H. Zhang, Y. Zhang, M. Yang, Characterization of unknown iodinated disinfection by-products during chlorination/chloramination using ultrahigh resolution mass spectrometry, Sci. Total Environ., 554–555 (2016) 83–88.
[21] Y. Pan, Y. Wang, A. Li, B. Xu, Q. Xian, C. Shang, P. Shi, Q. Zhou, Detection, formation and occurrence of 13 new polar phenolic chlorinated and brominated disinfection by-products in drinking water, Water Res., 112 (2017) 129–136.
[22] Y.M. Qi, N.N. Wu, Z.N. Tu, V.K. Sharma, Z.B. Wei, D.M. Zhou, Z.Y. Wang, R.J. Qu, Enhanced removal of ammonia in Fe(VI)/Br^- oxidation system: kinetics, transformation mechanism and theoretical calculations, Water Res., 222 (2022) 118953, doi: 10.1016/j.watres.2022.118953.
[23] Q. Zheng, N.N. Wu, R.J. Qu, G. Albasher, W.M. Cao, B.B. Li, N. Alsultan, Z.Y. Wang, Kinetics and reaction pathways for the transformation of 4-*tert*-butylphenol by ferrate(VI), J. Hazar. Mater., 401 (2020) 123405, doi: 10.1016/j.jhazmat.2020.123405.
[24] R. Prucek, J. Tucek, J. Kolarik, I. Hušková, J. Filip, R.S. Varma, V.K. Sharma, R. Zbořil, Ferrate(VI)-prompted removal of metals in aqueous media: mechanistic delineation of enhanced efficiency via metal entrenchment in magnetic oxides, Environ. Sci. Technol., 49 (2015) 2319–2327.
[25] M.B. Feng, X.H. Wang, J. Chen, R.J. Qu, Y.X. Sui, L. Cizmas, Z.Y. Wang, V.K. Sharma, Degradation of fluoroquinolone antibiotics by ferrate(VI): effects of water constituents and oxidized products, Water Res., 103 (2016) 48–57.
[26] J. Chen, N.N. Wu, X.X. Xu, R.J. Qu, C.G. Li, X.X. Pan, Z.B. Wei, Z.Y. Wang, Fe(VI)-mediated single-electron coupling processes for the removal of chlorophenol: a combined experimental and computational study, Environ. Sci. Technol., 52 (2018) 12592–12601.
[27] J.F. Zhao, Q. Wang, Y.S. Fu, B. Peng, G.F. Zhou, Kinetics and mechanism of diclofenac removal using ferrate(VI): roles of Fe^{3+}, Fe^{2+}, and Mn^{2+}, Environ. Sci. Pollut. Res., 25 (2018) 22998–23008.
[28] K. Manoli, G. Nakhla, M.B. Feng, V.K. Sharma, A.K. Ray, Silica gel-enhanced oxidation of caffeine by ferrate(VI), Chem. Eng. J., 330 (2017) 987–994.
[29] E. Neubauer, F.V.D. Kammer, T. Hofmann, Using FLOWFFF and HPSEC to determine trace metal-colloid associations in wetland runoff, Water Res., 47 (2013) 2757–2769.
[30] M.S. Rahman, G.A. Gagnon, Bench-scale evaluation of drinking water treatment parameters on iron particles and water quality, Water Res., 48 (2014) 137–147.

[31] B.C. Cao, B.Y. Gao, X. Liu, M.M. Wang, Z.L. Yang, Q.Y. Yue, The impact of pH on floc structure characteristic of polyferric chloride in a low DOC and high alkalinity surface water treatment, Water Res., 45 (2011) 6181–6188.
[32] J. Bridgeman, B. Jefferson, S.A. Parsons, Computational fluid dynamics modeling of flocculation in water treatment: a review, Eng. Appl. Comput. Fluid Mech., 3 (2009) 220–241.
[33] E. Gasparini, S.C. Tarantinoa, P. Ghignab, M.P. Riccardia, E.I. Cedillo-Gonzálezc, C. Siligardic, M. Zema, Thermal dehydroxylation of kaolinite under isothermal conditions, Appl. Clay Sci., 80–81 (2013) 417–425.
[34] M.B. Ogundiran, S. Kumar, Synthesis and characterization of geopolymer from Nigerian Clay, Appl. Clay Sci., 108 (2015) 173–181.

Supplementary information

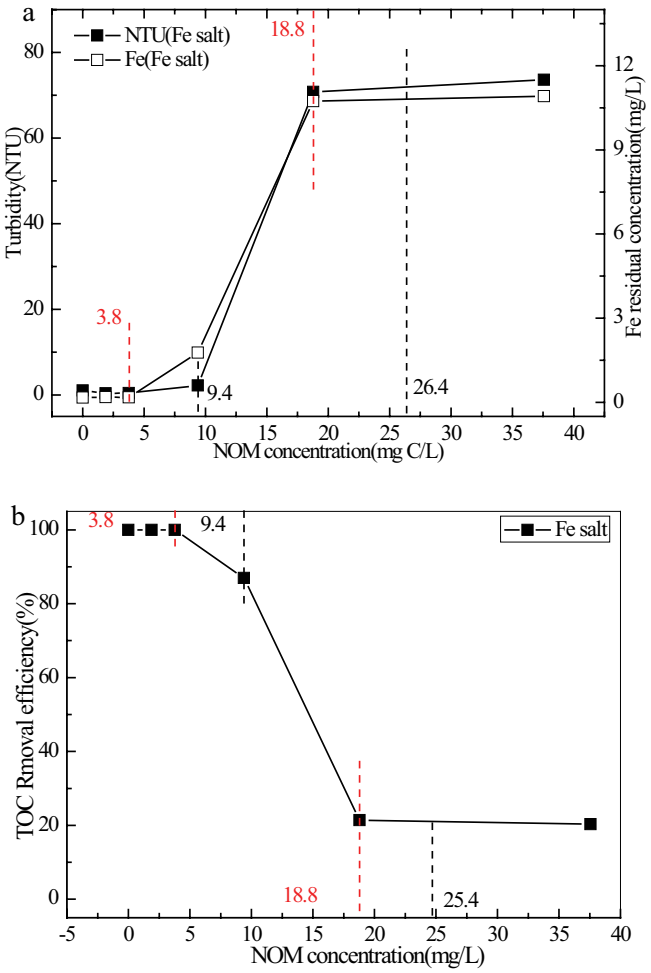

Fig. S1. Fe concentration and remaining turbidity (a), TOC removal efficiency (b) in the solution during the NOM removal by Fe salt (Fe salt dosage: 0.2 mM; NOM concentration: 0–40 mg/L; kaolin dosage: 50 mg/L; pH: 7.0).

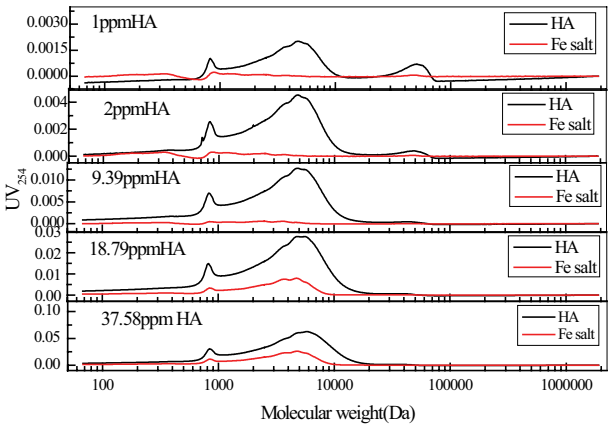

Fig. S2. HA molecular weight distribution after Fe salt treatment.

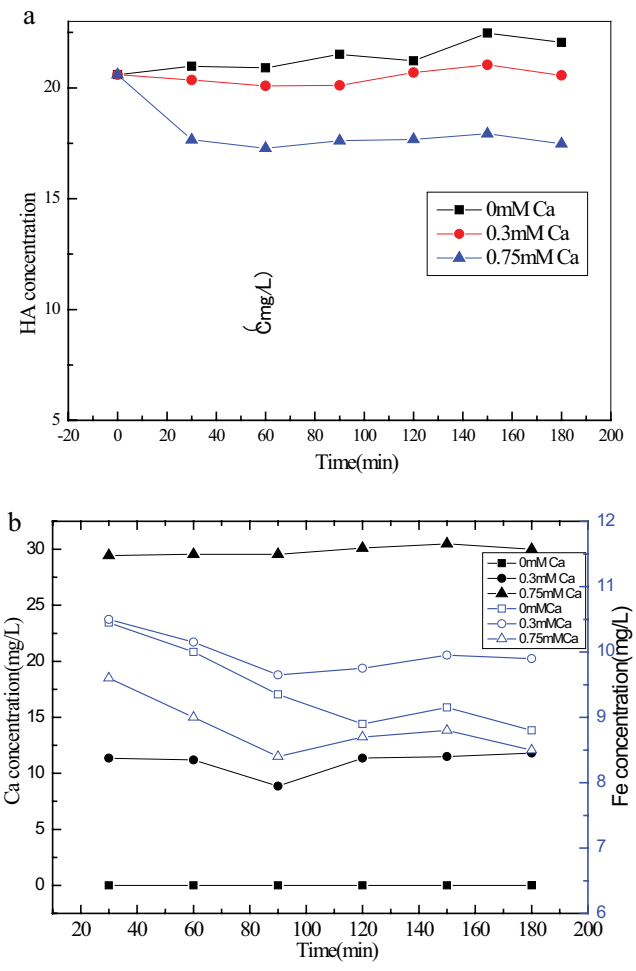

Fig. S3. TOC removal efficiency, Fe concentration and Ca concentration in the solution during the HA removal by ferrate (ferrate dosage: 0.2 mM; HA concentration: 21 mg/L; Ca dosage: 0–0.75 mM; pH: 9.0).

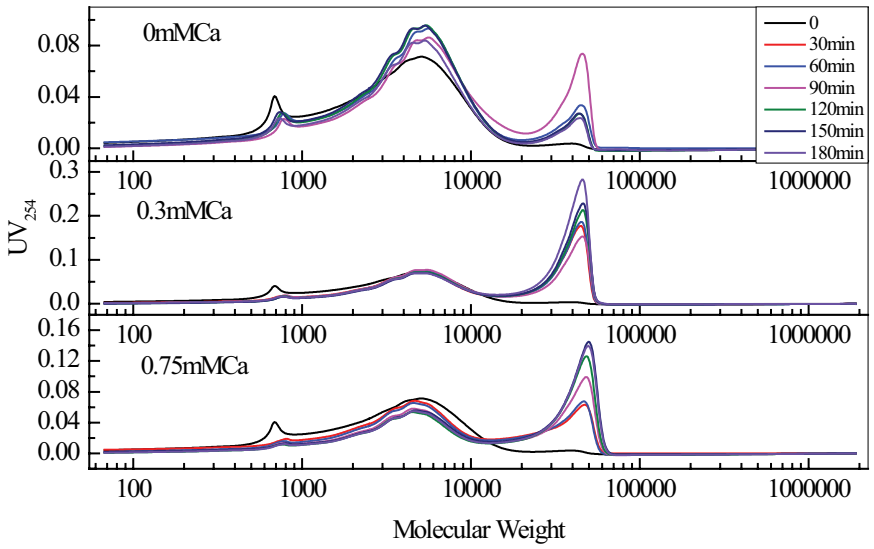

Fig. S4. HA molecular weight distribution after treatment by ferrate with Ca.